THE JOURNAL OF BIOLOGICAL CHEMISTRY VOL. 287, NO. 27, pp. 22740–22748, June 29, 2012

RUTBC2 Protein, a Rab9A Effector and GTPase-activating Protein for Rab36*

Received for publication, March 14, 2012, and in revised form, May 8, 2012 Published, JBC Papers in Press, May 25, 2012, DOI 10.1074/jbc.M112.362558

Ryan M. Nottingham[‡1], Ganesh V. Pusapati[‡], Ian G. Ganley[‡2], Francis A. Barr[§], David G. Lambright[¶], and Suzanne R. Pfeffer[‡3]

From the [‡]Department of Biochemistry, Stanford University School of Medicine, Stanford, California 94305, the [§]Department of Biochemistry, University of Oxford, Oxford OX1 3QU, United Kingdom, and the [¶]Department of Biochemistry and Molecular Pharmacology, University of Massachusetts Medical School, Worcester, Massachusetts 01605

Background: Rab GTPases control membrane traffic, and identification of Rab regulators is incomplete.
Results: RUTBC2 binds Rab9A, enhances GTP hydrolysis by Rab34 and Rab36 *in vitro*, and is a GAP for Rab36 in cells.
Conclusion: These data suggest a connection between Rab9A and Rab36 as part of a cascade of membrane traffic steps.
Significance: This represents the first assignment of a molecular function for RUTBC2.

Rab GTPases regulate vesicle budding, motility, docking, and fusion. In cells, their cycling between active, GTP-bound states and inactive, GDP-bound states is regulated by the action of opposing enzymes called guanine nucleotide exchange factors and GTPase-activating proteins (GAPs). The substrates for most RabGAPs are unknown, and the potential for cross-talk between different membrane trafficking pathways remains uncharted territory. Rab9A and its effectors regulate recycling of mannose 6-phosphate receptors from late endosomes to the trans Golgi network. We show here that RUTBC2 is a TBC domain-containing protein that binds to Rab9A specifically both *in vitro* and in cultured cells but is not a GAP for Rab9A. Biochemical screening of Rab protein substrates for RUTBC2 revealed highest GAP activity toward Rab34 and Rab36. In cells, membrane-associated RUTBC2 co-localizes with Rab36, and expression of wild type RUTBC2, but not the catalytically inactive, RUTBC2 R829A mutant, decreases the amount of membrane-associated Rab36 protein. These data show that RUTBC2 can act as a Rab36 GAP in cells and suggest that RUTBC2 links Rab9A function to Rab36 function in the endosomal system.

Rab GTPases are master regulators of membrane trafficking (1). They catalyze the formation of functional membrane microdomains by recruiting effectors to specific membranes while in their GTP-bound states. There are ~70 Rabs encoded by the human genome and likely ~40 expressed in any given cell (2). Rab effector proteins are defined as those that bind specific Rabs in their GTP-bound state (1). Effectors confer functionality to Rab proteins by recruiting motor proteins or serving as cargo adaptors and tethering factors to facilitate membrane trafficking. In cells, GTPase-activating protein (GAP)[4] proteins regulate the levels of GTP-bound Rab by greatly accelerating the intrinsic rate of GTP hydrolysis by a Rab (1). There are at least 40 human RabGAPs, suggesting that RabGAPs are highly specific for their Rab protein substrates (1).

RUTBC2 is a putative Rab GAP conserved in *Caenorhabditis elegans*, *Drosophila*, and vertebrates. The primary sequence of RUTBC2 reveals the presence of two domains, an N-terminal RPIP8/Unc-14/NESCA (RUN) domain and a C-terminal Tre-2/Bub2/Cdc16 (TBC) domain (1, 3–7). RUN domains are thought to function as protein-protein interaction domains, whereas TBC domains possess RabGAP activity and are conserved from yeast to humans.

Little is known about either the biochemistry or the cell biology of RUTBC2. It was first detected in purified lysosomal membranes in a study to find the causative factor of mucopolysaccharidosis IIIC, a disease with defective lysosomal enzyme activity (8). Later, Shimizu and co-workers (9) found RUTBC2 to have a more restricted expression pattern than the highly related RUTBC1; RUTBC2 was highly enriched in mouse brain. Furthermore, RUTBC2 was reported to localize to the trans Golgi network in mouse neuroblastoma cells (9). These authors also detected interaction of RUTBC2 with Rap1A/B and Rap2A/B via a region just C-terminal to the RUN domain. RUTBC2 thus seems to be a likely candidate for integrating signaling from Rap-regulated pathways to membrane trafficking. The Rab substrates of its putative GAP activity remain unknown.

Rab9A GTPase is required for the recycling of mannose 6-phosphate receptors from late endosomes to the trans Golgi network (10, 11). It also plays a role in lysosome biogenesis (12) and late endosome morphology (13). In this study, we report that RUTBC2 is a specific effector of Rab9A *in vitro* and in cultured cells. Rab9A binds the N-terminal half of RUTBC2. The RUTBC2 TBC domain does not possess GAP activity on Rab9A but instead shows *in vitro* GAP activity toward the

* This work was supported, in whole or in part, by National Institutes of Health Grant DK37332 (to S. R. P.).
[1] Supported in part by National Institutes of Health Training Grant GM007276.
[2] Present address: MRC Protein Phosphorylation Unit, University of Dundee, Dundee DD1 5EH, Scotland, United Kingdom.
[3] To whom correspondence should be addressed: Dept. of Biochemistry, Stanford University School of Medicine, 279 Campus Dr. B400, Stanford, CA 94305-5307. Tel.: 650-723-6169; Fax: 650-723-6783; E-mail: pfeffer@stanford.edu.

[4] The abbreviations used are: GAP, GTPase-activating protein; MDCC, *N*-[2-(1-maleimidyl)ethyl]-7-(diethylamino) coumarin-3-carboxamide; MPR, mannose 6-phosphate receptor; GTPγS, guanosine 5′-O-[y-thio]triphosphate; PBP, phosphate-binding protein; RUN, RPIP8/UNC-14/NESCA; TBC, Tre2/Bub2/Cdc16; VSV-G, vesicular stomatitis virus glycoprotein.

highly related Rab34 and Rab36 proteins. In cells, Rab36 is a *bona fide* substrate for RUTBC2.

EXPERIMENTAL PROCEDURES

Yeast Two-hybrid Analysis—Yeast two-hybrid analysis was carried out as described previously (14). Briefly, 56 mutant Rab proteins deficient for GTP hydrolysis (Gln to Ala) were cloned into pGBT9 bait vector (Clontech). RUTBC2 was amplified from cDNA libraries and was cloned into pACT2 prey vector (Clontech); growth on selective medium indicated an interaction between a Rab and RUTBC2.

Plasmids—For mammalian expression, N-terminally 3×Myc-tagged RUTBC2 was obtained by amplification from a cDNA library and ligation into a modified version of pCDNA3.1(+) (Invitrogen) (14). This construct encodes the shortest of four isoforms found in GenBank™ and is missing the first 25 amino acids at the N terminus. GFP-RUTBC2 was constructed by amplification of this isoform with the addition of the missing N terminus by PCR and ligated into pEGFP-C3 (Clontech). The predicted RUTBC2 GAP-inactive mutant (R829A) was created using QuikChange (Stratagene).

For bacterial expression, RUTBC2-N (amino acids 1–449) and RUTBC2-C (amino acids 450–1032) were ligated into pET28a (Novagen) in-frame with the N-terminal His tag or into the AscI and PacI sites of a modified pGEX-6P-1 vector (GE Healthcare) in-frame with an N-terminal GST tag. A plasmid encoding full-length GST-RUTBC2 was constructed by ligation of full-length RUTBC2 into pGEX-6P-1. Untagged Rab9CLLL, GST-Rab9A, and GST-Rab9A Q66L were described (15). His-Rab9A was ligated from untagged Rab9CLLL (15) and ligated into pET14b. His-Rab2 was amplified from pGBT9-Rab2 (14) and ligated into pET28a. GST-Rab9B was amplified by PCR from pET14-Rab9B (16) and ligated into pGEX-4T-1. His-Rab6A was described previously (17). GST-C110 and GST-C123 were previously described (18). pEGFP-Rab36 has been described (19). Myc-Rab9A Q66L was described previously (20). GFP-Rab9A has also been described previously (15).

Rab proteins tested for GAP activity were previously described (21). Phosphate-binding protein (PBP) from *Escherichia coli* was amplified by PCR from bacteria and cloned into modified pET15. His-PBP A197C was constructed by site-directed mutagenesis.

Protein Expression and Purification—Either His-RUTBC2-N or His-RUTBC2-C was transformed into Rosetta2 (DE3) cells (Novagen) and grown at 37 °C until $A_{600} = 0.5$. The culture was induced with 0.4 mM isopropyl β-D-thiogalactoside and grown for an additional 4 h at 22 °C. Cell pellets were resuspended in lysis buffer (25 mM HEPES, pH 7.4, 300 mM NaCl, 50 mM imidazole) supplemented with 1 mM PMSF and lysed by two passes at 20,000 p.s.i. through an EmulsiFlex-C5 apparatus (Avestin). Cleared lysates (20,000 rpm for 45 min at 4 °C in a JA-20 rotor; Beckman Coulter) were incubated with nickel-nitrilotriacetic acid (Qiagen) for 1 h at 4 °C. The resin was then washed with lysis buffer and eluted with 25 mM HEPES, pH 7.4, 300 mM NaCl, and 250 mM imidazole. Fractions containing the required protein were pooled and concentrated using an Amicon Ultra concentrator (Millipore). The sample was dialyzed to remove imidazole and then brought to 10% (v/v) glycerol. The sample was aliquoted, snap-frozen in liquid nitrogen, and stored at −80 °C. GST-RUTBC2, GST-RUTBC2-N, and GST-RUTBC2-C were each transformed into Rosetta2 (DE3) cells and grown at 37 °C until $A_{600} = 0.6$. The cells were induced with 100 μM isopropyl β-D-thiogalactoside and grown for an additional 4.5 h at 30 °C. Cell pellets were resuspended in lysis buffer (50 mM HEPES, pH 7.4, 250 mM NaCl, 1 mM DTT, 1 mM EDTA) supplemented with 1 mM PMSF and lysed by two passes at 20,000 p.s.i. through an EmulsiFlex-C5. Cleared lysates (19,000 rpm for 30 min at 4 °C in a JA-20 rotor; Beckman Coulter) were incubated with glutathione-Sepharose Fast Flow (GE Healthcare) for 1.5 h at 4 °C. The resin was then washed with 25 column volumes lysis buffer and eluted with 50 mM Tris-HCl, pH 8.0, 250 mM NaCl, and 20 mM glutathione. Fractions containing RUTBC2-C were pooled and concentrated using an Amicon Ultra concentrator (Millipore). The sample was dialyzed to remove glutathione and brought to 10%(v/v) glycerol, snap-frozen in liquid nitrogen, and stored at −80 °C.

Untagged Rab9CLLL, GST-Rab9A, and GST-Rab9A Q66L expression and purification were previously described (15), and GST-Rab9B was purified by the same procedure. His-Rab9A and His-Rab2 were purified in the same manner as His-Rab6A (16). Full activity (>50%) of all Rabs was verified by nucleotide binding (15). Expression and purification of GST-C110 and GST-C123 were previously described (18). Expression and purification of Rab proteins for the GAP screen were previously described (21). His-PBP A197C was purified and labeled with *N*-[2-(1-maleimidyl)ethyl]-7-(diethylamino)coumarin-3-carboxamide (MDCC) as described previously (22).

Antibodies—Mouse monoclonal anti-Myc (9E10), mouse monoclonal anti-Rab9A, mouse monoclonal anti-CI-MPR (2G11), and rabbit anti-CI-MPR were all previously described (23). Rabbit anti-GFP antibody was from Invitrogen; mouse anti-GFP antibody was from Roche Applied Science. Rabbit anti-RUTBC2 was purchased from Sigma. Anti-Penta-His antibody was from Qiagen. Chicken anti-Myc antibody was from Bethyl Laboratories. HRP-conjugated goat anti-mouse and goat anti-rabbit secondary antibodies as well as protein-A-HRP were from Bio-Rad.

Binding Assays—Constructs encoding 3×Myc-RUTBC2 were translated *in vitro* using a TNT quick coupled transcription/translation system (Promega) following the manufacturer's protocol. GST-tagged Rabs were loaded with GTPγS or GDP as described (15) and mixed with TNT lysate for 1.5 h at 25 °C in binding buffer (25 mM HEPES-NaOH, pH 7.4, 150 mM NaCl, 5 mM $MgCl_2$, 1 mM DTT, 0.1 mM GTPγS). RUTBC2 constructs bound to GST-Rabs were isolated using glutathione-Sepharose, washed in binding buffer (with 400 mM NaCl), and then eluted by the addition of 25 mM glutathione and analyzed by immunoblot. For binding described for Fig. 2*A*, 1 μM His-Rab2 and His-Rab9A was preloaded with GTPγS and incubated with 2.5 μM GST or full-length GST-RUTBC2 for 90 min at room temperature in binding buffer (50 mM HEPES, pH 7.4, 150 mM NaCl, 5 mM $MgCl_2$, 0.1 mg/ml BSA). Glutathione-Sepharose was added and incubated for 30 min at room temperature, and bound protein complexes were eluted by heating the sam-

ples in 2× Laemmli buffer and analyzed by immunoblotting with anti-His antibody. For binding described for Fig. 2, *B* and *F*, the Rab concentration was 5 μM, and the GST or GST-RUTBC2 concentration was 2.5 μM. Binding assays described for Fig. 2*D* using purified proteins were as described (16). For Fig. 2*E*, GST alone or GST-Rab9A Q66L (5 μM) was mixed with His-RUTBC2-N or His-RUTBC2-C (2.5 μM) and incubated for 1 h at 25 °C in binding buffer (25 mm HEPES, pH 7.4, 150 mM KCl, 5 mM $MgCl_2$, 0.1 mg/ml BSA). RUTBC2 constructs bound to GST and GST-Rab9A were isolated using glutathione-Sepharose, washed in binding buffer, eluted with 2× Laemmli buffer, and analyzed by immunoblotting with anti-His antibody.

Cell Culture and Transfections—HeLa, HEK293T, SK-N-SH, and Vero cells were obtained from American Type Culture Collection and cultured at 37 °C and 5% CO_2 in Dulbecco's modified Eagle's medium supplemented with 7.5% fetal calf serum, 100 units of penicillin, and 100 μg/ml streptomycin. For overexpression studies, all cells were transfected using FuGENE 6 (Roche Applied Science). Cells were harvested either 24 h or 48 h after transfection as indicated. For siRNA treatment, HEK293T cells were transfected using Lipofectamine 2000 (Invitrogen). The siRNA against RUTBC2 targeted the sequence 5′-GCAGAUUGGAGGAGAAACA-3′ and was purchased from Dharmacon.

Immunoprecipitation, Protein Turnover, Lysosomal Enzyme Secretion, and Fractionation—For immunoprecipitation, HEK293T cells overexpressing GFP-Rab9A and 3×Myc-RUTBC2 constructs were harvested after 24 h and lysed in lysis buffer (Tris-HCl, pH 7.4, 150 mM NaCl, 5 mM $MgCl_2$, 1 mM EDTA, 1 mM dithiothreitol, 1% Triton X-100, 10% glycerol, and 100 nM GTPγS) supplemented with 1 mM PMSF, 2.3 μM leupeptin, 1.5 μM pepstatin, and 150 nM aprotinin. After centrifugation at 12,000 × *g* for 10 min, protein concentrations were measured in the lysates. 1000 μg of extract was precleared with protein-A-Sepharose (GE Healthcare) at 4 °C for 60 min. The precleared extracts were incubated with GFP-binding protein-conjugated Sepharose (38) for 90 min at 4 °C. Immobilized proteins were washed with lysis buffer, eluted with 2× Laemmli buffer, and subjected to SDS-PAGE. Bound proteins were detected by immunoblotting. Protein turnover and lysosomal enzyme secretion assays were performed as described (23). Cell fractionation was as described previously (13) except that SK-N-SH cells were swollen in 10 mM HEPES, pH 7.4, for 5 min.

GAP Assays—The procedure followed by Pan *et al.* (21) was used, except that phosphate released during the reaction was bound by His-PBP A197C labeled at position 197 with MDCC (24). Reactions were started by adding a solution containing GAP and $MgCl_2$ to one of MDCC-PBP and desalted, GTP-exchanged Rabs by a Precision 2000 liquid handling system (BioTek). All reactions contained 2 μM Rab GTPase, 5 mM $MgCl_2$, and 85 nM MDCC-PBP, whereas the concentration of His-RUTBC2-C was varied. Phosphate production was monitored continuously in a TECAN Sapphire microplate reader using an excitation wavelength of 425 nm and an emission wavelength of 455 nm.

Immunofluorescence Microscopy—HeLa cells were seeded on glass coverslips and transfected the following day with FuGENE 6 (Promega). 18 h after transfection, cells were washed twice in PBS followed by two washes with ice-cold glutamate buffer (25 mM HEPES-NaOH, pH 7.4, 25 mM KCl, 2.5 mM magnesium acetate, 5 mM EGTA, and 150 mM monopotassium glutamate). Cytosol leak was performed by incubating the coverslips for 5 s in liquid N_2 and thawing them at 20 °C for 1 min. Coverslips were then washed twice in ice-cold glutamate buffer and fixed for 15 min in 3.7% paraformaldehyde in 200 mM HEPES-NaOH, pH 7.4. After fixation, cells were washed twice in PBS and permeabilized with 0.1% Triton X-100 in PBS for 3 min. Coverslips were washed twice in PBS, blocked with 1% BSA in PBS (blocking buffer) for 30 min, incubated with chicken anti-Myc antibody diluted in blocking buffer for 1 h at 20 °C, washed, incubated with Alexa Fluor 555 or Alexa Fluor 594 (Invitrogen) secondary antibody diluted in blocking buffer for 1 h, and then washed and mounted using Mowiol (Polysciences). Imaging was performed with a Leica TCS SP2 SE confocal scanner in conjunction with a Leica DM6000 B upright scope (with attached Leica HCX PL apochromatic 63×/NA 1.4 objective) and a Leica CTR 6000 confocal control box. This setup was controlled by Leica Control software (Leica Microsystems). Images were processed using ImageJ. The quantification of Rab36 puncta and fluorescence intensity as well as Rab9A and RUTBC2 co-localization was performed with CellProfiler.

RESULTS

We are interested in understanding the cellular role of Rab9A GTPase. As a starting point to find regulators of Rab9A, we used a yeast two-hybrid screen consisting of all TBC domain-containing proteins in the human genome as prey against a comprehensive library of hydrolysis-deficient Rab GTPases as bait (14, 25). This screen revealed that a TBC domain-containing protein, RUTBC2, interacted with both Rab9A and Rab9B (Fig. 1*B*). RUTBC2 also interacted with Rab2A/B and Rab7li.

According to the National Center for Biotechnology Information (NCBI) HomoloGene database, there is only one RUTBC1/2 protein in *C. elegans* (tbc-8), *Drosophila* (CG1905), and zebrafish (LOC794373), whereas vertebrates have both RUTBC1 and RUTBC2 proteins (9). Unlike most other GAP proteins, the TBC catalytic domains of RUTBC1 and RUTBC2 contain a large insertion between the first two "fingerprint" A and B motifs (Fig. 1*A*, sequence). These motifs are unambiguously conserved in all TBC domains (1) and comprise the catalytic core of these enzymes. What is the role of the sequences that interrupt the catalytic core? In the structural model for Rab and Rab-GAP interaction, the analogous region of Gyp1 GAP is situated away from the Rab-GAP binding interface (21), thus these large insertions may have important binding interactions related to the functions of these proteins. Most of the dissimilarity between RUTBC1 and RUTBC2 in the TBC domain is found in this insertion; thus, these sequences are likely to contribute to the different functions of RUTBC1 and RUTBC2.

RUTBC2 Is a Rab9A Effector—To confirm the results of the screen and to test the nature of the interactions, we tested whether Rab9A could bind RUTBC2 *in vitro*. Full-length RUTBC2 was produced both in an *in vitro* transcription/translation system (with an N-terminal 3×Myc tag) as well as in

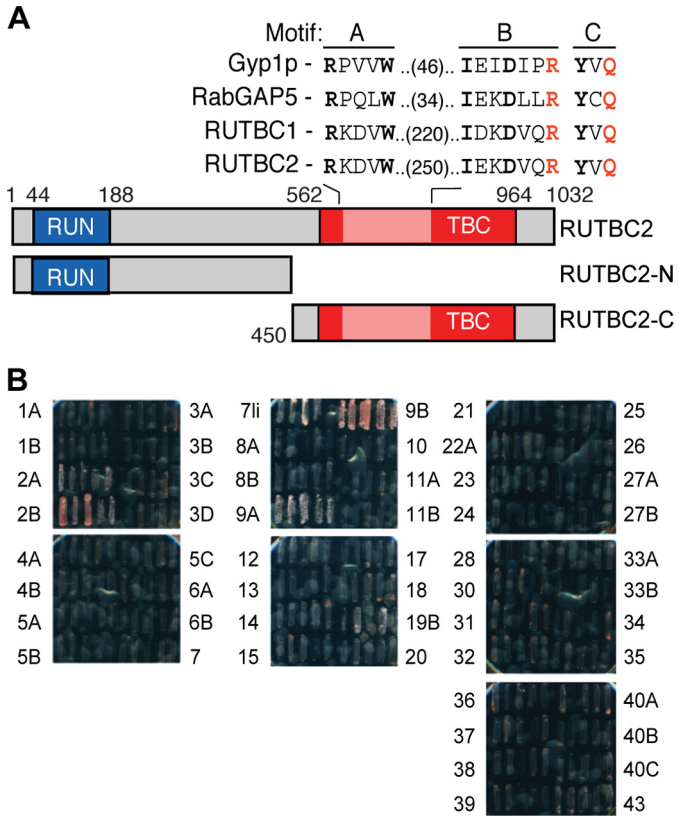

FIGURE 1. **RUTBC2 interacts with Rab9.** *A*, diagram of RUTBC2 domain structure. The RUN domain is shown in *blue*; the TBC domain is shown in *red*. The first three conserved motifs of the TBC domain are indicated at the *top*. Conserved residues are in *bold*, and the predicted catalytic arginine and glutamine are shown in *red*, respectively. The extended insert between motif A and motif B of RUTBC2 is compared with the same regions of human RUTBC1 and RabGAP-5 (RUTBC3) and *Saccharomyces cerevisiae* Gyp1p. The structures of RUTBC2-N (residues 1–449) and RUTBC2-C (450–1032) are shown. *B*, RUTBC2 was screened against a library of 56 human Rab GTPases. Growth after streaking on selective medium indicates an interaction between RUTBC2 and a Rab GTPase.

E. coli (with an N-terminal GST tag). As shown in Fig. 2*A*, His-Rab9A bound well to GST-RUTBC2 and not GST, whereas another Rab that showed interaction in the two-hybrid screen, Rab2A, did not bind either GST or GST-RUTBC2. GST-RUTBC2 bound to His-Rab9A but not to His-Rab6A (Fig. 2*B*). Next, we asked whether RUTBC2 preferred either the GTP-bound or the GDP-bound form of Rab9A. Using the GST binding assay described above, *in vitro* translated RUTBC2 was bound much more efficiently by GST-Rab9A when loaded with GTPγS as compared with GDP (Fig. 2*C*). These results also suggest that RUTBC2 prefers to bind Rab9A despite Rab9B interaction observed in the two-hybrid screen. Thus, RUTBC2 is a *bona fide* effector of Rab9A.

We next investigated the location of the Rab9A binding site in RUTBC2. Using purified proteins, full-length GST-RUTBC2 bound to Rab9A at levels comparable with the positive control for Rab9A binding: the GST-tagged, C-terminal 110 amino acids of GCC185 protein (21) (Fig. 2*D*). 5-fold less Rab9A bound to the negative control, the GST-tagged C-terminal 123 amino acids of Golgin245 (Fig. 2*D*). Rab9A bound poorly to the TBC domain alone (His-tagged RUTBC2-C terminus or RUTBC2-C) but very well to His-tagged RUTBC2-N representing the N-terminal half; only background binding was detected for GST-Rab9A binding to RUTBC2-C (Fig. 2*E*). His-Rab9A bound comparably to RUTBC2 full-length and RUTBC2-N constructs (Fig. 2*F*). This suggests that the N-terminal half is available for binding in the context of the full-length protein. An earlier two-hybrid screen for GAP-Rab interactions failed to detect Rab9A binding to RUTBC2 (26). This was very likely due to the use of constructs lacking non-TBC domain sequences. Taken together, these data demonstrate that Rab9A binds directly to RUTBC2 in its N-terminal half.

RUTBC2 Interacts with RAB9A in Cells—RAB9A regulates the recycling of mannose 6-phosphate receptors (MPRs) from late endosomes to the trans Golgi network (10–12). To test whether Rab9A and RUTBC2 interact in cells, HEK293T cells were transfected with 3×Myc-RUTBC2 and GFP or GFP-Rab9A. Using GFP-binding protein-conjugated Sepharose to precipitate these proteins, we detected the presence of 3×Myc-RUTBC2 in immunoprecipitates of GFP-Rab9A but not GFP (Fig. 3*A*). Thus, RUTBC2 can interact with Rab9A in living cells.

We further characterized this interaction by investigating the effects of exogenously expressed RUTBC2 on MPR recycling. When Rab9A function is disturbed in cells by overexpression of a dominant negative mutant Rab9A (12) or by depletion of its effectors (18, 20, 27), MPRs are missorted to the lysosome. We reasoned that if RUTBC2 had GAP activity on Rab9A, the phenotype of RUTBC2 overexpression should be similar to that of a GDP-preferring Rab9A mutant or Rab9A depletion.

When RUTBC2 was overexpressed in COS-1 cells, MPR levels at steady state were decreased by ~40% (Fig. 3*B*). This observation led us to investigate the turnover rate of MPR in HeLa cells overexpressing RUTBC2, and we found it to be essentially unchanged (Fig. 3*C*). This suggested that although some amount of MPRs was being missorted to lysosomes, there was likely a decrease in MPR transcription or translation. In a functional test of MPR trafficking, we measured the amount of hexosaminidase activity secreted into the medium by cells transfected with RUTBC2. Hexosaminidase is usually sorted to the lysosome, but when MPR levels are deficient in the trans Golgi network due to missorting events, the hydrolase is secreted. In 293T cells transfected with RUTBC2, slightly higher hexosaminidase activity was detected in the medium than in control cells (Fig. 3*D*). Cells transfected with a catalytically inactive protein, RUTBC2 R829A, showed a similar effect. Taken together, perturbation of MPR trafficking is likely due to titration of Rab9A by the overexpression of RUTBC2 rather than the GAP activity of this protein.

Further proof that Rab9A interacts with RUTBC2 in HeLa cells comes from experiments in which expression of the activated, GTP-locked form of Rab9A, Rab9A Q66L, led to increased localization of RUTBC2 to membrane compartments that harbor Rab9A (Fig. 4). In cells transfected with wild type Rab9A, very little co-localization between Rab9A and RUTBC2 was observed (~10%). In contrast, 78% of RUTBC2-positive structures were also positive for Rab9A Q66L ($n = 700$). Thus, RUTBC2 binds Rab9A in a variety of cell types.

RUTBC2 Has Narrow Substrate Specificity—Identification of the Rab substrates of RUTBC2 should provide important insight regarding its cellular function and the significance of the

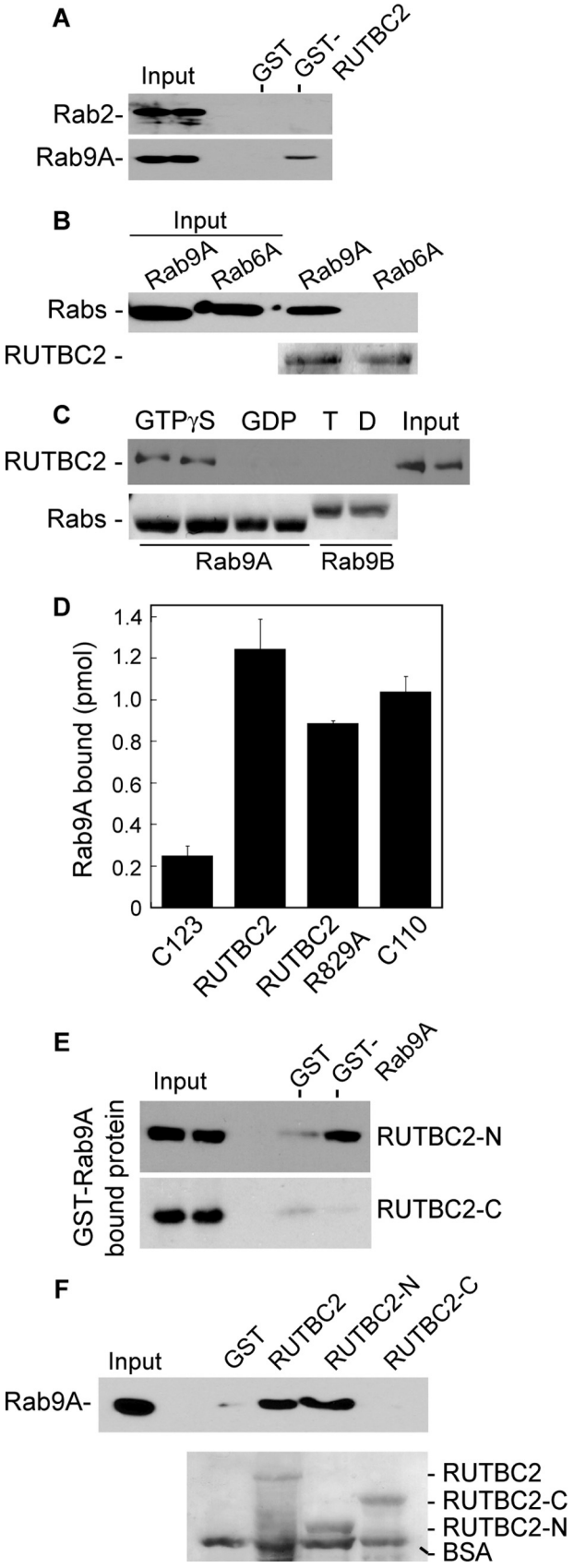

FIGURE 2. **RUTBC2 is an effector of Rab9A.** *A*, His-Rab2 and His-Rab9A were preloaded with GTPγS and incubated with GST or full-length GST-RUTBC2 and then collected on glutathione-Sepharose. Bound material was eluted in sample buffer and analyzed by immunoblot with anti-His antibodies. Inputs represent 5% of the added His-tagged Rab. *B*, His-Rab9A and His-Rab6A were preloaded with GTPγS and incubated with full-length GST-RUTBC2 and then collected on glutathione-Sepharose. Bound material was eluted in sample buffer and analyzed by immunoblot with anti-His antibodies. Inputs represent 10% of the added His-tagged Rabs. *C*, *in vitro* transcribed/translated 3×Myc-RUTBC2 was incubated with GST-Rab9A or GST-Rab9B preloaded with either GTPγS (*T*) or GDP (*D*) and analyzed as in *A*. *D*, purified GST-RUTBC2 and control proteins were incubated with untagged Rab9A loaded with [^{35}S]GTPγS and immobilized using glutathione-Sepharose. Bound Rab was detected by scintillation counting. *Error bars* represent S.E. from at least two independent experiments. *E*, His-RUTBC2-N or His-RUTBC2-C was incubated with GST or GST-Rab9A Q66L and then collected on glutathione-Sepharose. Bound material was eluted in sample buffer and analyzed by immunoblot using anti-His antibodies. Inputs represent 5% of the added His-tagged RUTBC2 constructs. *F*, His-Rab9A was preloaded with GTPγS and incubated with GST, full-length GST-RUTBC2, GST-RUTBC2-N, or GST-RUTBC2-C and then collected on glutathione-Sepharose. Bound material was eluted in sample buffer and analyzed by immunoblot with anti-His antibodies. Inputs represent 5% of the added His-tagged Rab.

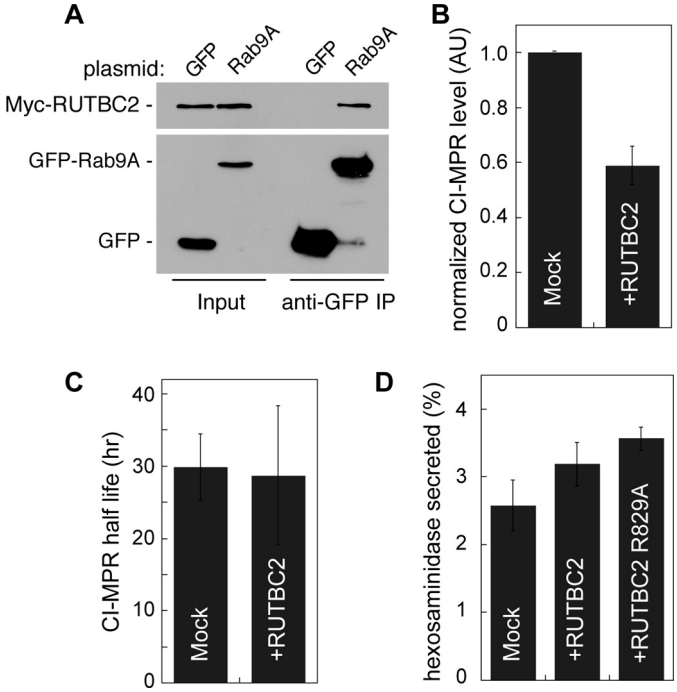

FIGURE 3. **RUTBC2 binds to, but is not a GAP for Rab9A in cells.** *A*, HEK293T cells were transfected with 3×Myc-RUTBC2 and GFP or GFP-Rab9A for 24 h, and GFP was immunoprecipitated with GFP-binding protein-conjugated Sepharose and immunoblotted with anti-Myc antibodies (*top panel*) and anti-GFP antibodies (*bottom panel*). *Input* represents 2% of the lysate subjected to immunoprecipitation. *B*, COS-1 cells were transfected with 3×Myc-RUTBC2 for 48 h, and total cell extracts were immunoblotted with anti-CI-MPR antibodies. *AU*, arbitrary units. *C*, quantitation of CI-MPR half-life measured from pulse-chase analysis of HeLa cells transfected with 3×Myc-RUTBC2 for 48 h. Extracts were immunoprecipitated with anti-CI-MPR antibodies and exposed to a phosphor screen. *D*, HEK293T cells transfected with 3×Myc-RUTBC2 wild type or R829A for 24 h were assayed for secreted and intracellular hexosaminidase activity. *Error bars* in *panels B–D* represent S.E. from at least two independent experiments.

Rab9A-RUTBC2 interaction. 32 different mammalian Rab GTPases were screened under single turnover conditions as substrates for RUTBC2 using purified, His-tagged RUTBC2-C that contains the catalytic TBC domain. Fig. 5 summarizes these results by comparing observed second order rate constants for GAP-catalyzed hydrolysis with the rate constants for intrinsic hydrolysis by each Rab protein. The TBC domain of RUTBC2 had the highest activity against Rab36 and Rab34, whereas no activity was detected against Rab9A or Rab2. There

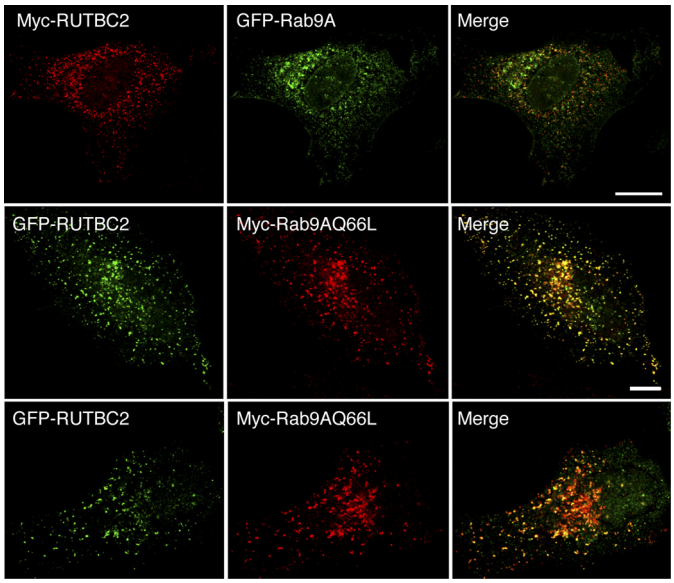

FIGURE 4. **RUTBC2 co-localizes with Rab9A Q66L.** *Upper panels*, confocal micrographs of HeLa cells co-expressing Myc-RUTBC2 and GFP-Rab9A. *Middle* and *lower panels*, confocal micrographs of GFP-RUTBC2 and Myc-Rab9A Q66L. The merged micrographs are shown in the *right column*. *Bar*, 10 μm.

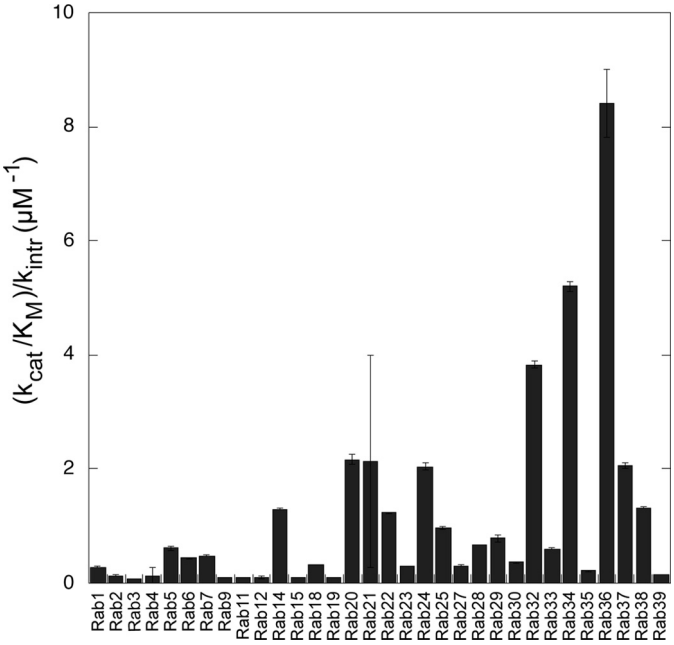

FIGURE 5. **RUTBC2 TBC domain has GAP activity toward Rab36 and Rab34 *in vitro*.** 32 purified, mammalian Rab GTPases were preloaded with GTP for 1 h at room temperature and then desalted to remove free nucleotide. Rabs were diluted with MDCC-PBP and mixed with $MgCl_2$ containing varying concentrations of purified His-RUTBC2-C to start the reaction. Phosphate release was monitored continuously by microplate fluorometer (see "Experimental Procedures"). Catalytic efficiency (k_{cat}/K_m) relative to the intrinsic rate constant (k_{intr}) for GTP hydrolysis was determined. Plots represent the mean from duplicate wells. The Rab isoforms used in the screen were the ubiquitously expressed isoforms; Rab9A was assayed. *Error bars* represent S.E. from at least two independent experiments.

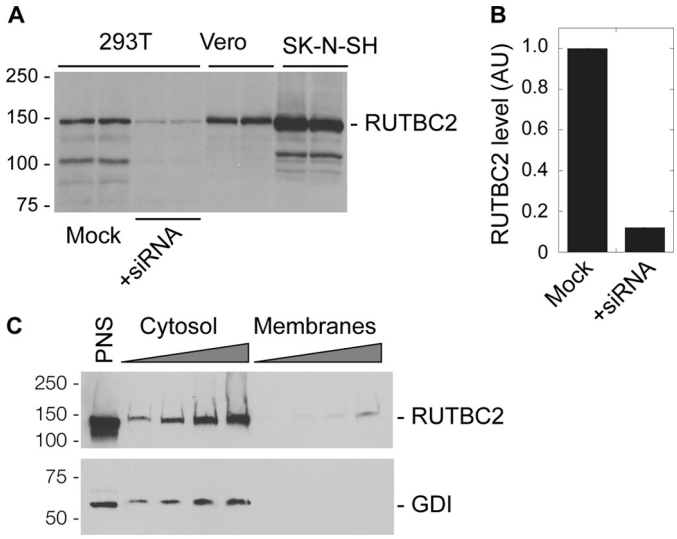

FIGURE 6. **Endogenous RUTBC2 is stably associated with membranes in SK-N-SH cells.** *A*, detergent extracts (100 μg) of indicated cell lines were resolved by SDS-PAGE and immunoblotted using anti-RUTBC2 antibodies. *B*, HEK293T cells were either mock-transfected or transfected with siRNA targeting RUTBC2 for 72 h. Shown is quantitation of the band corresponding to RUTBC2. *AU*, arbitrary units. *C*, SK-N-SH cells were fractionated into crude membranes and cytosol. Increasing volumes of each fraction were analyzed by immunoblot using RUTBC2-specific antibodies. *PNS*, postnuclear supernatant.

was also activity toward Rab32, which is a substrate for the closely related RUTBC1 (28). Both Rab36 and Rab34 are reported to be localized to the Golgi (29, 30), but little else is known about their precise roles. Additionally, His-Rab2 was tested as a substrate for full-length RUTBC2; no enhancement of GTP hydrolysis rate was detected in reactions containing up to equimolar amounts of Rab2 and RUTBC2 proteins (data not shown).

RUTBC2 Is Enriched in Neural Cells—Analysis of different cell lines revealed that RUTBC2 is present in different amounts in HEK293T, Vero, and SK-N-SH cells (Fig. 6*A*). SK-N-SH cells are a human neuroblastoma cell line that might be similar to the mouse Neuro2a neuroblastoma cells used by Shimizu and coworkers (9) in earlier RUTBC2 studies. RUTBC2 was highly expressed in these cells as compared with kidney cells, consistent with that study. RUTBC2 could be efficiently depleted by siRNA treatment of 293T cells (Fig. 6*B*). Quantitation revealed approximately ~90% depletion. Fractionation of SK-N-SH cells showed that most RUTBC2 was cytosolic. Nevertheless, a small amount of RUTBC2 stably associated with membranes (Fig. 6*C*). Unfortunately, the antibody could not be used for immunofluorescence microscopy to determine the specific membranes with which endogenous RUTBC2 associates.

RUTBC2 Acts on Rab36 in Cells—To test whether Rab34 or Rab36 are substrates for RUTBC2 in cells, GFP-tagged Rabs were co-expressed with RUTBC2 or a catalytically inactive RUTBC2 R829A mutant protein. As described earlier, most RUTBC2 is cytosolic (Fig. 6*C*). To remove the cytosolic pool and permit detection of RUTBC2 on membranes, cells were frozen in liquid nitrogen to break membranes and washed to deplete cytosol prior to fixation.

When expressed alone, GFP-tagged Rab36 protein localized to ~125 punctate structures per cell (Fig. 7*A*, *top panel*). These did not contain late endosomal MPRs or Rab9A, lysosomal LAMP-1, early endosomal EEA1, early or recycling endosomal transferrin, or the Golgi protein, GM130 (not shown). We conclude that Rab36 is present in a distinct class of endosomal structures.

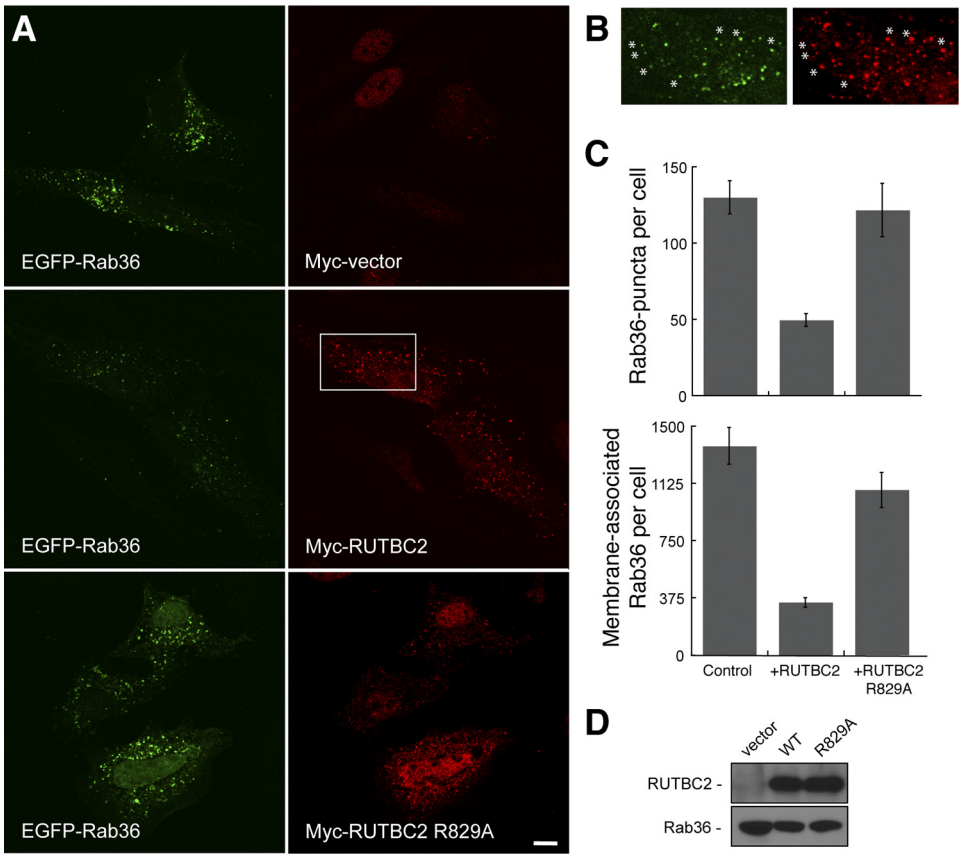

FIGURE 7. **RUTBC2 is a GAP for Rab36 in cells.** *A*, confocal micrographs (with identical exposure times) of HeLa cells co-expressing EGFP-Rab36 and Myc-empty vector (*upper panels*), 3×Myc-RUTBC2 (*middle panel*), or 3×Myc-RUTBC2 R829A (*lower panel*). *Bar*, 10 μm. *B*, enlargement of the *boxed area* from the corresponding *middle panels* of Fig. 6*A*, with brightness increased to display co-localization of EGFP-Rab36 (*left*) and Myc-RUTBC2 (*right*). *Asterisks* are included to facilitate identification of co-localized puncta. *C*, quantification of the number of Rab36 puncta and their fluorescence intensity as a measure of membrane-associated Rab36 protein. Data represent the average of two experiments ($n = 40$ cells). *Error bars* represent S.E. of two independent experiments. *D*, HeLa cells were co-transfected as in *A*, and total cell extracts were immunoblotted for RUTBC2 and Rab36 using anti-Myc and anti-GFP antibodies, respectively.

RUTBC2 protein was detected on the same cytosolic puncta that were labeled with GFP-Rab36 (Fig. 7*A*, *middle panels* shown enlarged in Fig. 7*B*). However, when catalytically active, wild type RUTBC2 protein was present, less Rab36 was seen on those structures as determined by quantification of the fluorescence intensity and the number of Rab36-positive puncta in each cell (Fig. 7, *A* and *C*). The level of Rab36 on vesicles did not change in cells in which similar levels of RUTBC2-R829A protein were expressed (Fig. 7, *A* and *C*). Importantly, immunoblot analysis of transfected cells showed that under all conditions tested, the cells expressed comparable amounts of Rab36 and either wild type or mutant RUTBC2 proteins (Fig. 7*D*).

Analogous experiments carried out with GFP-Rab34 failed to reveal any change in localization upon expression of RUTBC2 protein (not shown). Together, these data demonstrate that RUTBC2 is a GAP for Rab36 in cells and suggest a model where RUTBC2 in some way links Rab9A function to Rab36-controlled pathways.

DISCUSSION

Here we have shown that a predicted RabGAP protein, RUTBC2, is a novel Rab9A effector. RUTBC2 does not display GAP activity on Rab9A but instead has GAP activity for Rab34 and Rab36 *in vitro* and acts on Rab36 in cells. RUTBC2 is present in many cell types but is enriched in cells of neural origin. A small pool of RUTBC2 also stably associates with membranes, which appear to represent a distinct class of endosome in HeLa cells. Although Rab9B appeared to interact with RUTBC2 in a two-hybrid screen, only purified Rab9A bound directly to RUTBC2. Binding to either Rab would be consistent with the observation that at least in some cell types, murine RUTBC2 localizes to the trans Golgi network (9) or to endosomes (this study). Rab9B is localized to the Golgi (19), whereas Rab9A regulates the transport of MPRs from late endosomes to the trans Golgi network. It is not yet clear precisely where Rab9A and RUTBC2 interact.

It is interesting to contrast the substrate specificity of RUTBC2 with that of RUTBC1 (28). RUTBC1 shows GAP activity toward Rab32 and Rab33B *in vitro* but only toward Rab32 in cells. RUTBC2 also displays GAP activity toward Rab32 but much less than RUTBC1 and shows no activity toward Rab33B. Because most of the sequence divergence between the two proteins occurs in the TBC domain between the A and B motifs, it would be interesting to compare structural models of the two proteins to see whether this region may fold back and contact the Rab substrates. The co-crystal of Gyp1p and Rab33B suggests that this region does not contact the Rab (21), but in this region, the RUTBC proteins are almost five times longer.

Currently, there are no known direct links between Rab9A-mediated trafficking and either Rab36-regulated or Rab34-regulated events. However, both Rab36 and Rab34 are thought to influence the localization of lysosomes (29, 30). GTP-restricted Rab34 or Rab36 causes LAMP1-positive lysosomes (and not MPR-positive structures) to cluster in the perinuclear area (29, 30, 31). This phenomenon is mediated by Rab-interacting lysosomal protein (RILP), an effector of both Rab34 and Rab36 as well as Rab7, a Rab known to play a role in lysosomal biogenesis. A mutation in the switch I region of Rab34 (K82Q) that blocks association with RILP fails to redistribute lysosomes (29). Little else is known about Rab36 other than the fact that it is deleted in many cases of malignant rhabdoid tumors (32).

Rab34 has also been suggested to play an additional role in constitutive secretion. It binds to hmunc-13, a diacylglycerol-binding protein (33). Depletion of Rab34 and hmunc-13 from HeLa cells blocks temperature-sensitive vesicular stomatitis virus glycoprotein (VSV-G) arrival at the plasma membrane (31, 34). Brefeldin A treatment revealed that blocked VSV-G returned to the endoplasmic reticulum, suggesting that Rab34 depletion causes a block in intra-Golgi transport rather than exit from the trans Golgi network (31). A previous screen for the ability of overexpressed RabGAPs to block VSV-G secretion in multiple cell types showed that RUTBC2 had no effect on this process (35). This suggests that RUTBC2 may only have activity on Rab36 in living cells, consistent with the data presented herein.

RUTBC2 has also been shown to interact with Nurr1, an orphan nuclear receptor required for the development of dopaminergic neurons in the mouse brain (36). Co-expression of RUTBC2 and Nurr1 increased transcription of endogenous tyrosine hydroxylase, part of the dopamine synthesis pathway (36). Moreover, suppression of RUTBC2 by siRNA led to decreased cell division and decreased expression of the dopamine transporter, a Nurr1 target gene (36). This has led to speculation that RUTBC2 may be important in the pathogenesis of Parkinson disease, which is influenced by Nurr1 (37).

There is currently no known connection between Nurr1 and Rab36. One attractive, but highly speculative, possibility might be that Rab36 is required for proper trafficking of the dopamine transporter. Further work will be needed to clarify the link between Rab9A, RUTBC2, Rab36, and Nurr1 and may enhance our understanding of the etiology of Parkinson disease.

REFERENCES

1. Barr, F., and Lambright, D. G. (2010) Rab GEFs and GAPs. *Curr. Opin. Cell Biol.* **22,** 461–470
2. Nguyen, U. T., Guo, Z., Delon, C., Wu, Y., and Deraeve C, Fränzel, B., Bon, R. S., Blankenfeldt, W., Goody, R. S., Waldmann, H., Wolters, D., and Alexandrov, K. (2009) Analysis of the eukaryotic prenylome by isoprenoid affinity tagging. *Nat. Chem. Biol.* **5,** 227–235
3. Callebaut, I., de Gunzburg, J., Goud, B., and Mornon, J. P. (2001) RUN domains: a new family of domains involved in Ras-like GTPase signaling. *Trends Biochem. Sci.* **26,** 79–83
4. Janoueix-Lerosey, I., Pasheva, E., de Tand, M. F., Tavitian, A., and de Gunzburg, J. (1998) Identification of a specific effector of the small GTP-binding protein Rap2. *Eur. J. Biochem.* **252,** 290–298
5. Recacha, R., Boulet, A., Jollivet, F., Monier, S., Houdusse, A., Goud, B., and Khan, A. R. (2009) Structural basis for recruitment of Rab6-interacting protein 1 to Golgi via a RUN domain. *Structure* **17,** 21–30
6. Neuwald, A. (1997) A shared domain between a spindle assembly checkpoint protein and Ypt/Rab-specific GTPase activators. *Trends Biochem. Sci.* **22,** 243–244
7. Strom, M., Vollmer, P., Tan, T. J., and Gallwitz, D. (1993) A yeast GTPase-activating protein that interacts specifically with a member of the Ypt/Rab family. *Nature* **361,** 736–739
8. Ausseil, J., Landry, K., Seyrantepe, V., Trudel, S., Mazur, A., Lapointe, F., and Pshezhetsky, A. V. (2006) An acetylated 120-kDa lysosomal transmembrane protein is absent from mucopolysaccharidosis IIIC fibroblasts: a candidate molecule for MPS IIIC. *Mol. Genet. Metab.* **87,** 22–31
9. Yang, H., Sasaki, T., Minoshima, S., and Shimizu, N. (2007) Identification of three novel proteins (SGSM1, 2, 3) which modulate small G protein (RAP and RAB)-mediated signaling pathway. *Genomics* **90,** 249–260
10. Lombardi, D., Soldati, T., Riederer, M. A., Goda, Y., Zerial, M., and Pfeffer, S. R. (1993) Rab9 functions in transport between late endosomes and the trans Golgi network. *EMBO J.* **12,** 677–682
11. Barbero, P., Bittova, L., and Pfeffer, S. R. (2002) Visualization of Rab9-mediated vesicle transport from endosomes to the trans Golgi in living cells. *J. Cell Biol.* **156,** 511–518
12. Riederer, M. A., Soldati, T., Shapiro, A. D., Lin, J., and Pfeffer, S. R. (1994) Lysosome biogenesis requires Rab9 function and receptor recycling from endosomes to the trans Golgi network. *J. Cell Biol.* **125,** 573–582
13. Ganley, I. G., Carroll, K., Bittova, L., and Pfeffer, S. (2004) Rab9 GTPase regulates late endosome size and requires effector interaction for its stability. *Mol. Biol. Cell* **15,** 5420–5430
14. Fuchs, E., Haas, A. K., Spooner, R. A., Yoshimura, S., Lord, J. M., and Barr, F. A. (2007) Specific Rab GTPase-activating proteins define the Shiga toxin and epidermal growth factor uptake pathways. *J. Cell Biol.* **177,** 1133–1143
15. Aivazian, D., Serrano, R. L., and Pfeffer, S. (2006) TIP47 is a key effector for Rab9 localization. *J. Cell Biol.* **173,** 917–926
16. Hayes, G. L., Brown, F. C., Haas, A. K., Nottingham, R. M., Barr, F. A., and Pfeffer, S. R. (2009) Multiple Rab GTPase binding sites in GCC185 suggest a model for vesicle tethering at the trans Golgi. *Mol. Biol. Cell* **20,** 209–217
17. Burguete, A. S., Fenn, T. D., Brunger, A. T., and Pfeffer, S. R. (2008) Rab and Arl GTPase family members cooperate in the localization of the golgin GCC185. *Cell* **132,** 286–298
18. Reddy, J. V., Burguete, A. S., Sridevi, K., Ganley, I. G., Nottingham, R. M., and Pfeffer, S. R. (2006) A functional role for the GCC185 golgin in mannose 6-phosphate receptor recycling. *Mol. Biol. Cell* **17,** 4353–4363
19. Yoshimura, S., Egerer, J., Fuchs, E., Haas, A. K., and Barr, F. A. (2007) Functional dissection of Rab GTPases involved in primary cilium formation. *J. Cell Biol.* **178,** 363–369
20. Espinosa, E. J., Calero, M., Sridevi, K., and Pfeffer, S. R. (2009) RhoBTB3: a Rho GTPase-family ATPase required for endosome to Golgi transport. *Cell* **137,** 938–948
21. Pan, X., Eathiraj, S., Munson, M., and Lambright, D. G. (2006) TBC-domain GAPs for Rab GTPases accelerate GTP hydrolysis by a dual-finger mechanism. *Nature* **442,** 303–306
22. Shutes, A., and Der, C. J. (2005) Real-time *in vitro* measurement of GTP hydrolysis. *Methods* **37,** 183–189
23. Ganley, I. G., Espinosa, E., and Pfeffer, S. R. (2008) A syntaxin 10-SNARE complex distinguishes two distinct transport routes from endosomes to the trans Golgi in human cells. *J. Cell Biol.* **180,** 159–172
24. Brune, M., Hunter, J. L., Corrie, J. E., and Webb, M. R. (1994) Direct, real-time measurement of rapid inorganic phosphate release using a novel fluorescent probe and its application to actomyosin subfragment 1 ATPase. *Biochemistry* **33,** 8262–8271
25. Haas, A. K., Fuchs, E., Kopajtich, R., and Barr, F. A. (2005) A GTPase-activating protein controls Rab5 function in endocytic trafficking. *Nat. Cell Biol.* **7,** 887–893
26. Itoh, T., Satoh, M., Kanno, E., and Fukuda, M. (2006) Screening for target Rabs of TBC (Tre-2/Bub2/Cdc16) domain-containing proteins based on their Rab-binding activity. *Genes Cells* **11,** 1023–1037
27. Díaz, E., Schimmöller, F., and Pfeffer, S. R. (1997) A novel Rab9 effector required for endosome-to-TGN transport. *J. Cell Biol.* **138,** 283–290
28. Nottingham, R. M., Ganley, I. G., Barr, F. A., Lambright, D. G., and Pfeffer, S. R. (2011) RUTBC1 protein, a Rab9A effector that activates

GTP hydrolysis by Rab32 and Rab33B proteins. *J. Biol. Chem.* **286,** 33213–33222
29. Wang, T., and Hong, W. (2002) Interorganellar regulation of lysosome positioning by the Golgi apparatus through Rab34 interaction with Rab-interacting lysosomal protein. *Mol. Biol. Cell* **13,** 4317–4332
30. Chen, L., Hu, J., Yun, Y., and Wang, T. (2010) Rab36 regulates the spatial distribution of late endosomes and lysosomes through a similar mechanism to Rab34. *Mol. Membr. Biol.* **27,** 24–31
31. Goldenberg, N. M., Grinstein, S., and Silverman, M. (2007) Golgi-bound Rab34 is a novel member of the secretory pathway. *Mol. Biol. Cell* **18,** 4762–4771
32. Mori, T., Fukuda, Y., Kuroda, H., Matsumura, T., Ota, S., Sugimoto, T., Nakamura, Y., and Inazawa, J. (1999) Cloning and characterization of a novel *Rab*-family gene, *Rab36*, within the region at 22q11.2 that is homozygously deleted in malignant rhabdoid tumors. *Biochem. Biophys. Res. Commun.* **254,** 594–600
33. Speight, P., and Silverman, M. (2005) Diacylglycerol-activated Hmunc13 serves as an effector of the GTPase Rab34. *Traffic* **6,** 858–865
34. Goldenberg, N. M., and Silverman, M. (2009) Rab34 and its effector munc13-2 constitute a new pathway modulating protein secretion in the cellular response to hyperglycemia. *Am. J. Physiol. Cell Physiol.* **297,** C1053–C1058
35. Haas, A. K., Yoshimura, S., Stephens, D. J., Preisinger, C., Fuchs, E., and Barr, F. A. (2007) Analysis of GTPase-activating proteins: Rab1 and Rab43 are key Rabs required to maintain a functional Golgi complex in human cells. *J. Cell Sci.* **120,** 2997–3010
36. Luo, Y., Xing, F., Guiliano, R., and Federoff, H. J. (2008) Identification of a novel Nurr1-interacting protein. *J. Neurosci.* **28,** 9277–9286
37. Federoff, H. J. (2009) Nur(R1)turing a notion on the etiopathogenesis of Parkinson disease. *Neurotox. Res.* **16,** 261–270
38. Rothbauer, U., Zolghadr, K., Muyldermans, S., Schepers, A., Cardoso, M. C., and Leonhardt, H. (2008) A versatile nanotrap for biochemical and functional studies with fluorescent fusion proteins. *Mol. Cell Proteomics* **7,** 282–289